**Article ID**: 1000-7032(2020)09-1114-08

# Enhancing Single-band Red Upconversion Luminescence of $Ho^{3+}$ Through Dye-sensitization

WANG Dan[1,2,3], XUE Bin[1,3], TU Lang-ping[3], ZHANG You-lin[3], SONG Jun[1*], QU Jun-le[1], KONG Xiang-gui[3*]

(1. *Key Laboratory of Optoelectronic Devices and Systems of Ministry of Education and Guangdong Province, College of Physics and Optoelectronic Engineering, Shenzhen University, Shenzhen* 518060, *China*;
2. *College of Information Engineering, Shenzhen University, Shenzhen* 518060, *China*;
3. *State Key Laboratory of Luminescence and Applications, Changchun Institute of Optics, Fine Mechanics and Physics, Chinese Academy of Sciences, Changchun* 130033, *China*)

* *Corresponding Authors, E-mail: songjun@szu.edu.cn; xgkong14@ciomp.ac.cn*

**Abstract**: Single-band red upconversion emission has important applications for high-resolution biomarkers and 3-dimensional color display. However, the cross-relaxation of $Ho^{3+}/Ce^{3+}$ co-doping system normally yield the weak single-band red emission. In this paper, the dye-sensitized $NaYF_4$: Yb/Ho/Ce (20%/2%/10%) @ $NaYF_4$: Nd (20%) nanoparticles were prepared to address such an issue. Highly uniform upconversion nanoparticles were prepared by solvothermal method, and the single-band red emission was obtained by increasing the $Ce^{3+}$ doping concentration (from 0% to 10%) inside the core. When the near-infrared dyes of IR-806 were further conjugated, the upconversion luminescence intensity exhibited a 22-fold enhancement, and the red-to-green emission ratio also increased from 4.8 to 8.4. This paper provides a new way to improve the intensity and the purity of single-band red upconversion luminescence through dye sensitization, which is beneficial to high-resolution bioimaging.

**Key words**: upconversion luminescence; single-band red emission; dye-sensitization; nanoparticles
**CLC number**: O482.31 **Document code**: A **DOI**: 10.37188/fgxb20204109.1114

# 染料敏化增强 $Ho^{3+}$ 单带上转换红光

王 丹[1,2,3], 薛 彬[1,3], 涂浪平[3], 张友林[3], 宋 军[1*], 屈军乐[1], 孔祥贵[3*]

(1. 深圳大学物理与光电工程学院 光电子器件与系统教育部/广东省重点实验室, 广东 深圳 518060;
2. 深圳大学 信息工程学院, 广东 深圳 518060;
3. 中国科学院长春光学精密机械与物理研究所 发光学及应用国家重点实验室, 吉林 长春 130033)

**摘要**: 单带上转换红光发射在高分辨生物标记及三维彩色显示方面具有重要应用。本文针对 $Ho^{3+}/Ce^{3+}$ 共掺杂纳米体系单带上转换红光较弱的问题,设计制备了染料(IR-806)敏化的 $NaYF_4$: Yb/Ho/Ce(20%/2%/10%) @ $NaYF_4$: Nd(20%)纳米晶,显著增强了上转换红光发射。采用溶剂热法制备了均匀的上转换纳米粒子,通过调控核内部 $Ce^{3+}$ 离子掺杂浓度比例(0~10%)逐步获得单带上转换红光发射。在此基础上,通过上

**收稿日期**: 2020-05-26; **修订日期**: 2020-06-27
**基金项目**: 国家重点基础研究发展计划(2018YFC0910602); 国家自然科学基金(11874354,11874355,61605130,11604331,61775145,61835009);吉林省科技厅自然科学基金(20180101222JC); 深圳市基础研究项目(JCYJ20180305125425815)资助
Supported by National Key R&D Program of China (2018YFC0910602); National Natural Science Foundation of China (11874354,11874355,61605130,11604331,61775145,61835009); Project of Science and Technology Agency of Jilin Province (20180101222JC); Shenzhen Basic Research Project(JCYJ20180305125425815)

转换纳米粒子表面连接近红外 IR-806 染料分子,808 nm 激发下其上转换发光强度提高了约 22 倍,特别地,红绿荧光强度比从 4.8 增至 8.4。结果表明,染料敏化可用于增强上转换单带红光发射,并提高红光色纯度,这有利于高清晰的生物成像应用。

**关　键　词**: 上转换发光; 单带红光发射; 染料敏化; 纳米粒子

## 1 Introduction

Lanthanide ions($Ln^{3+}$), characterized by unique $4f^n$ electronic configuration, can generate the radiative emission ranging from the ultraviolet to the infrared region[1-2]. Especially, $Ln^{3+}$-doped upconversion nanoparticles(UCNPs) can convert two or more low-energy near-infrared photons into high-energy ultraviolet/visible photons. Their features of the large anti-Stokes shift, narrow emission band, long luminescence lifetime[3-4], could find promising applications in bioimaging, photodynamic therapy and display devices[5-8]. Moreover, due to that biological tissues have weak light scattering and absorption for near-infrared(NIR) light, NIR-excited upconversion luminescence is of particular interest in biomedicine[9-10].

As well known, single-band red emission has excellent applications in 3D full-color display and high-resolution bioimaging[11]. At present, to achieve the bright single-band red emission, Yb/Er codoping systems were most widely studied by further doping with $Mn^{2+}$ or $Tm^{3+}$ ions. In such systems, doping ions could induce the cross-relaxation process with $Er^{3+}$, leading to the quenching of the green emission and consequent increase of the red to green(R/G) emission ratio[12-14]. Similarly, introducing $Ce^{3+}$ ions into the Yb/Ho upconversion luminescence system could also cause the cross-relaxation process and increase the R/G luminescence intensity ratio[15]. However, the obtained single-band red upconversion emission is normally weak, which is unfavorable for the following applications such as high resolution of biological imaging. Although the cross-relaxation strategy could produce the single band red emission, the total upconversion luminescence(UCL) was greatly reduced. Therefore, how to produce single-band red emission while simultaneously maintaining the UCL intensity becomes a critical issue need to be addressed.

In this paper, we reported the preparation of the dye-sensitized $NaYF_4$: Yb/Ho/Ce(20%/2%/10%)@$NaYF_4$: Nd(20%) nanoparticles towards enhanced single-band red upconversion luminescence of $Ho^{3+}$. The UCNPs were first prepared through a facile solvothermal method, and then conjugated with the dye molecules of IR-806. The UCL was studied by varying the doping concentration of $Ce^{3+}$.

## 2 Experiments

### 2.1 Synthesis of UCNPs

$NaYF_4$: Yb/Ho/Ce(20%/2%/$x$%, $x$=0, 3, 5, 7, 10)@$NaYF_4$: Nd(20%) core/shell nanoparticles were synthesized according to previous reports[16-17]. For synthesizing 0.5 mmol samples, $YCl_3 \cdot 6H_2O$(99.9%, 0.395, 0.38, 0.37, 0.36, 0.345 mmol), $CeCl_3 \cdot 6H_2O$(99.9%, 0, 0.015, 0.025, 0.035, 0.05 mmol), $YbCl_3 \cdot 6H_2O$(99.9%, 0.1 mmol) and $HoCl_3 \cdot 6H_2O$(99.9%, 0.005 mmol) were dispersed in a solution containing 3 mL of OA and 7.5 mL of ODE. The suspension was first heated at 155 ℃ for 0.5 h to get a clear *Ln*-OA complex solution. Then $NH_4F$(2 mmol) and NaOH(1.25 mmol) dissolved in 6 mL of methanol were added to the reaction solution. Afterwards, the solution was heated to 70 ℃ to remove the methanol and subsequently heated at 300 ℃ for 1 h. After that, 1 mmol of $NaYF_4$: Nd(20%) active shell solution was injected into the above reaction mixture and maintained 15 min for ripening. Finally, the solution was cooled down to room temperature and precipitated using ethanol for three times.

### 2.2 Synthesis of IR-806 Modified UCNPs

According to the reported methods[18-19], the IR-780 dye molecule was first carboxylated to obtain the IR-806 dye. Dimethylformamide(10 mL), IR-

780 molecule (250 mg), 4-mercaptobenzoic acid (115.5 mg) were mixed and dissolved. After reaction for 17 h under argon, the solution was filtered and distilled under reduced pressure to remove dimethylformamide. The obtained product was re-dissolved in 5 mL of dichloromethane, followed by further filtration, precipitation with glacial ether and vacuum drying. The resulting product was IR-806 and was kept in the dark for use. For surface conjugation of UCNPs with dyes, the obtained 1 mL IR-806 (2 mg/mL) and 10 mg $NaYF_4$: Yb/Ho/Ce (20%/2%/10%) @ $NaYF_4$: Nd(20%) nanoparticles (dissolve in chloroform), were mixed and stirred at room temperature under dark conditions for 24 h, then centrifuged and re-dispersed in 1 mL of chloroform. Finally, the surface-modified UCNPs of IR-806 were diluted 200-fold for further spectroscopic analysis.

### 2.3 Characterizations

The power X-ray diffraction (XRD) patterns of the UCNPs were recorded on a Rigaku Miniflex 600 bench top powder X-ray diffraction instrument with Cu-Kα ($\lambda$ = 0.154 nm) radiation, operating at 40 kV and 15 mA. The morphology and particle size distributions of the samples were also checked using a FEI Tecnai G220 transmission electron microscope (TEM). Fourier transform infrared (FTIR) spectra were recorded with 2 $cm^{-1}$ resolution (Paragon 1000, Perkin-Elmer, USA). The room-temperature photoluminescence emission spectra were measured on a Horiba Fluoromax-3 fluorometer upon excitation with a continuous 808 nm fiber coupled diode lasers. The absorption spectra were acquired on a Maya 2000 spectrometer (Ocean Optics).

## 3 Results and Discussion

### 3.1 Characterizations of Nanoparticles

As shown in Fig. 1, transmission electron microscopy showed that UCNPs were uniform in size and the particle size was approximately 31 nm. XRD data showed (Fig. 2(a)) that the diffraction peaks of the prepared nanoparticles were in agreement with the standard $NaYF_4$ hexagonal phase pattern (JCPDS: 16-0334), confirmed that the prepared nanoparticles were hexagonal phase structure. Next, the IR-806 dye was prepared by carboxylation of a commercially available IR-780 dye (Fig. 2(b)). As shown in Fig. 2(c), the absorption peak of the dye molecule was centered at 806 nm, confirming that the IR-806 dye was successfully prepared. On the other hand, the infrared absorption spectra analysis of the structure of dye-sensitized UCNPs (UCNPs@dye) also confirmed the success of conjugating dyes on the surface of UCNPs. Fig. 2(d) shows the FTIR spectra of the obtained UCNPs and UCNPs@dye. Due to the presence of oleic acid ligands on the surface of UCNPs, infrared vibration peaks of 2 929 and 2 850 $cm^{-1}$ were observed, which correspond to the symmetry and antisymmetric vibrations of the methylene group of the oleic acid ligands, respectively. After further conjugation with the IR-806 molecules, in addition to the vibration modes of oleic acid molecules, a new vibration peak appeared at 1 251 $cm^{-1}$ for UCNPs@dye, which corresponded to the C-O stretching mode of IR-806. The appearance of this new vibration peak suggested that IR-806 molecules were coordinated on the surface of UCNPs

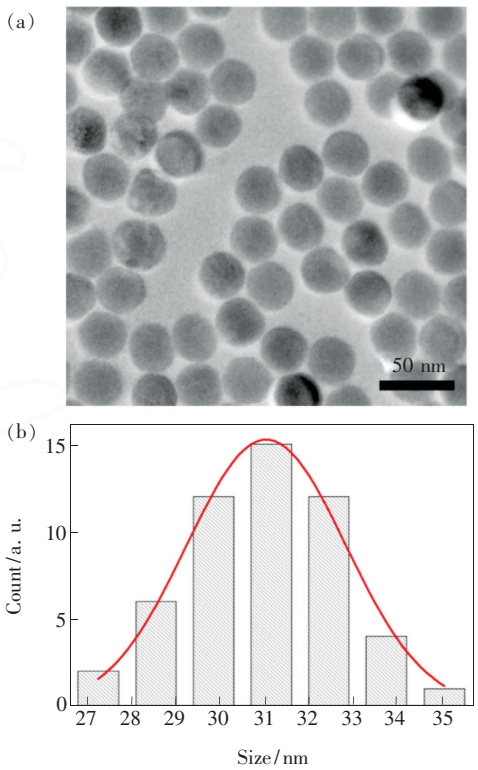


Fig. 1 (a) TEM image of $NaYF_4$: Yb/Ho/Ce (20%/2%/10%) @ $NaYF_4$: Nd(20%) upconversion nanoparticles. (b) Size distribution of UCNPs.

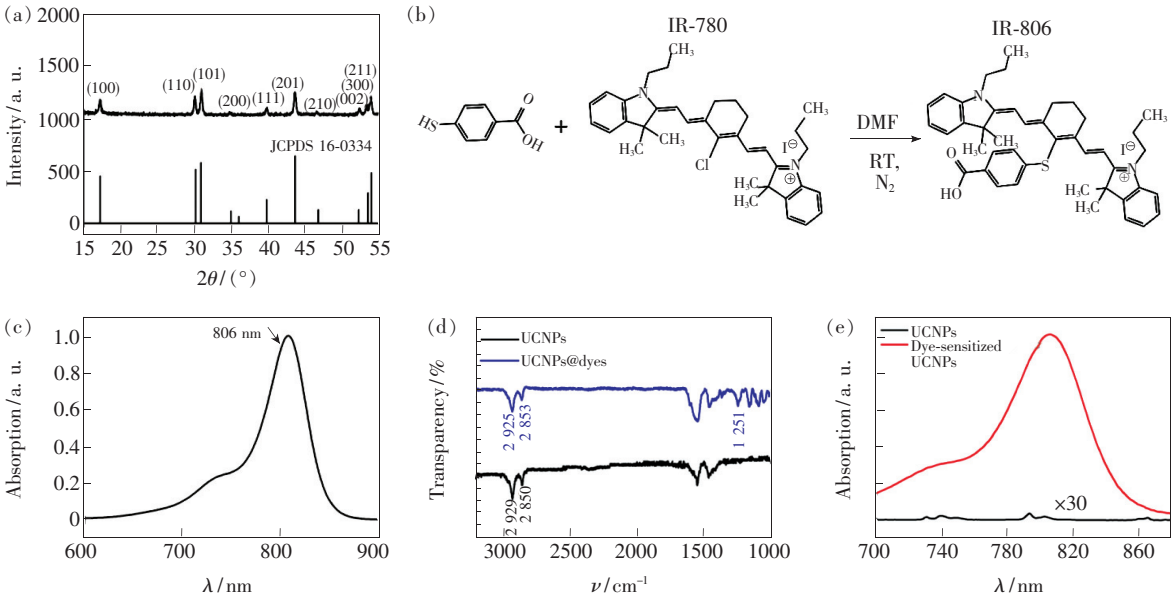


Fig. 2　(a) XRD patterns of UCNPs and the standard card of β-$NaYF_4$ (JCPDS-16-0334). (b) Synthesis process of IR-806. (c) Absorption spectrum of IR-806. (d) FTIR spectra of UCNPs and UCNPs@ dye. (e) Absorption spectra of UCNPs and dye-sensitized UCNPs.

*via* carboxyl group. Moreover, a broad absorption peak (~806 nm) appeared well following that of dye conjugation, which further indicated the successful synthesis of UCNPs@ dye.

### 3.2　Upconversion Luminescence of $Ho^{3+}$ in $NaYF_4$: Yb/Ho/Ce@$NaYF_4$: Nd Nanopartices

The designed $NaYF_4$: Yb/Ho/Ce@ $NaYF_4$: Nd (20%) nanostructure could produce the single-band upconversion red emission upon 808 nm excitation due to the cross-relaxation (CR) strategy between $Ho^{3+}$ and $Ce^{3+}$. According to previous reports[20-21], the $Nd^{3+}$ ions sensitized core-shell nanostructure was adopt to avoid the quenching effects between the activators and $Nd^{3+}$ ions. The $Nd^{3+}$-shell could suppress the surface-related quenching and further transfer excitation energy to the activators located in the inner core for UCL. Fig. 3(a) shows the luminescence spectra of $NaYF_4$: Yb/Ho/Ce(20%/2%/$x$%, $x$ = 0, 3, 5, 7, 10)@ $NaYF_4$: Nd(20%) UCNPs. The green emission (540 nm) and the red emission(645 nm) originating from the $^5S_2$, $^5F_4 \rightarrow {}^5I_8$ and $^5F_5 \rightarrow {}^5I_8$ transitions of $Ho^{3+}$ respectively, were observed. As shown in Fig. 3(e), the luminescence mechanism follows the first energy migration from $Nd^{3+}$ to $Ho^{3+}$ *via* $Yb^{3+}$, and subsequent energy transfer upconversion (ETU) with $^5I_6$ as the metastable level. Fig. 3(b) shows that as the $Ce^{3+}$ doping concentration increased, the R/G emission ratio gradually increased. In addition, as shown in Fig. 3(c), the overall upconversion luminescence intensity gradually decreased with increasing $Ce^{3+}$ doping concentration. Moreover, as shown in Fig. 3(d), the Commission Internationale de L'Eclairage (CIE) chromaticity coordinate (calculated using the colorimetry system as suggested in the CIE 1931) of the upconversion luminescence of different samples also indicated that the luminescence gradually moved from the green to the red region. According to previous report[15], the observed luminescence evolution with $Ce^{3+}$ doping could be reasonably explained as being due to the three CR processes (Fig. 3(e)): CR1: $^5I_6$ ($Ho^{3+}$) + $^2F_{5/2}$ ($Ce^{3+}$) $\rightarrow {}^5I_7$ ($Ho^{3+}$) + $^2F_{7/2}$ ($Ce^{3+}$), CR2: $^5S_2/{}^5F_4$ ($Ho^{3+}$) + $^2F_{5/2}$ ($Ce^{3+}$) $\rightarrow$ $^5F_5$ ($Ho^{3+}$) + $^2F_{7/2}$ ($Ce^{3+}$), CR3: $^5F_5$ ($Ho^{3+}$) + $^2F_{5/2}$ ($Ce^{3+}$) $\rightarrow {}^5I_4$ ($Ho^{3+}$) + $^2F_{7/2}$ ($Ce^{3+}$). The CR process induced by $Ce^{3+}$ was more effective to quench the green emission of $Ho^{3+}$ than red emission, resulting in a significant increase in the R/G emission ratio (Fig. 3(b)). However, the effective CR process also greatly decreased the overall UCL intensity, as shown in Fig. 3(c), more than 90% of

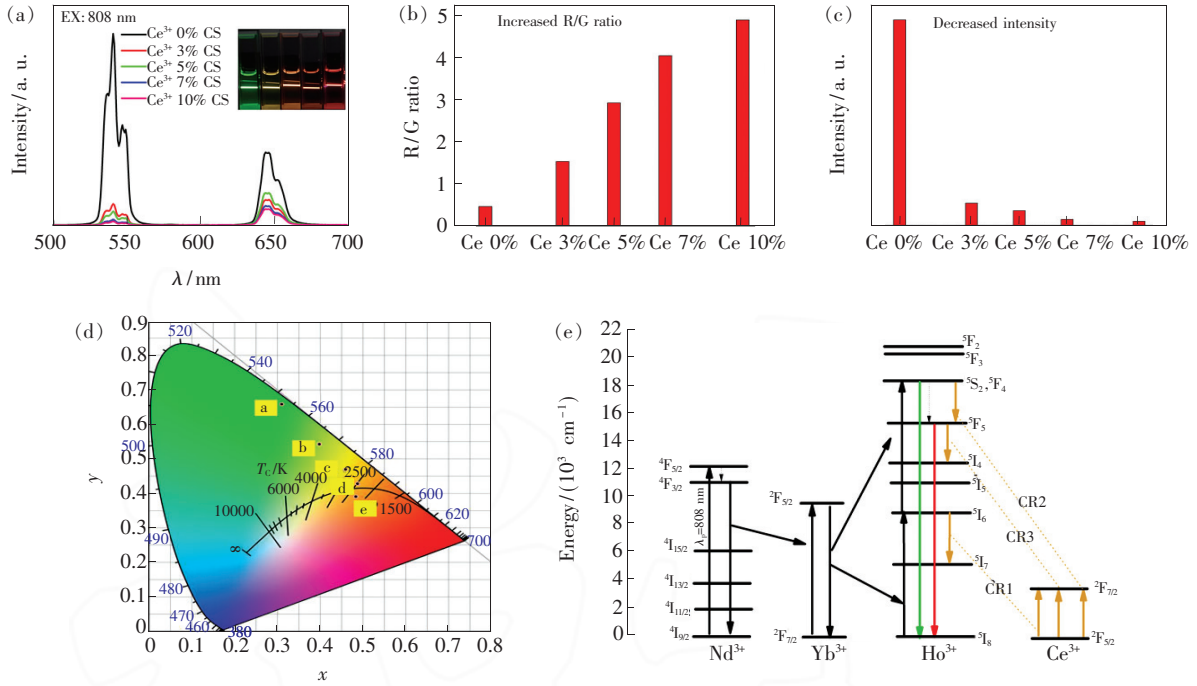


Fig. 3 (a) UC luminescence spectra of the samples of $NaYF_4$: Yb/Ho/Ce (20%/1%/$x$%, $x$ = 0, 3, 5, 7, 10) @ $NaYF_4$: Nd (20%) UCNPs under 808 nm excitation. The increased R/G (b) and the decreased luminescence intensity (c) with the doping concentration of $Ce^{3+}$. (d) CIE chromaticity diagram of the samples with different $Ce^{3+}$ concentrations (a – e corresponding to $x$ = 0, 3, 5, 7, 10). (e) Schematic diagram of the energy levels and the proposed UC mechanism.

UC emission was quenched when doping 10% $Ce^{3+}$. Therefore, how to maintain the intensity of single-band red upconversion luminescence becomes an issue needed to be addressed.

### 3.3 Upconversion Luminescence of $NaYF_4$: Yb/Ho/Ce@$NaYF_4$: Nd@dye

To achieve the enhancement of single-band red upconversion luminescence, we designed and prepared the dye-sensitized $NaYF_4$: Yb/Ho/Ce (20%/2%/10%) @ $NaYF_4$: Nd (20%) UCNPs, where the $Nd^{3+}$ ions located in outer layer served as energetic acceptors from IR-806 before further transferring the excitation energy to the internal luminescence centers, due to the fact that $Nd^{3+}$ ions have multiple absorption bands overlapping with the emission of the near-infrared dyes of IR-806[19-20]. As shown in Fig. 4(a), the single-band red upconversion luminescence of UCNPs was enhanced by a factor of 22. Similar to our previous report[19], this significant upconversion luminescence enhancement was mainly attributed to the strong near-infrared light absorption ability of the conjugated dye molecules. The dyes could transfer a large amount of absorbed excitation energy to $Nd^{3+}$, and then further to the internal luminescent centers, as a consequence, the upconversion luminescence was enhanced greatly. It should be noted that, as shown in Fig. 4(b), the dye-sensitization also increased the R/G emission ratio of $Ho^{3+}$ from 4.9 to 8.4. According to our previous publication[22], such results could be explained as bellow. When the slope of the power-dependent multi-photon processes of the red emission was larger than that of green emission, the R/G emission ratio increased with excitation power density. Herein, dye sensitization played a role of increasing excitation power due to their larger absorption cross-section at the excitation wavelength, then it could increase the R/G emission ratio under the equivalent excitation power density. We tested the power-dependent multi-photon processes of the $NaYF_4$: Yb/Ho/Ce (20%/2%/10%) @ $NaYF_4$: Nd (20%) UCNPs. Fig. 4(c) shows the double logarithm plot resulting

from the luminescence intensity *versus* pump power density, where the slope values of *n* for the $^5S_2$, $^5F_4 \rightarrow {}^5I_8$ (540 nm) and $^5F_5 \rightarrow {}^5I_8$ (645 nm) transitions of the $Ho^{3+}$ ions were 2.0, 1.9, respectively. The slope of the red emission was larger than that of green emission. The same case holds for the dye-sensitized $NaYF_4$: Yb/Ho/Ce (20%/2%/10%) @ $NaYF_4$: Nd(20%) UCNPs (Fig. 4(d)). It is obvious that the intensity of the red emission increases faster than the green emission with the excitation power density. Therefore, the R/G will gradually increase with the excitation power density. The effect of dye-sensitization is similar to increase the excitation power[22], and could therefore increase the R/G ratio. Therefore, dye-sensitization not only increased the intensity of single-band red upconversion luminescence of $Ho^{3+}$, but also improved the red purity of the UC emission.

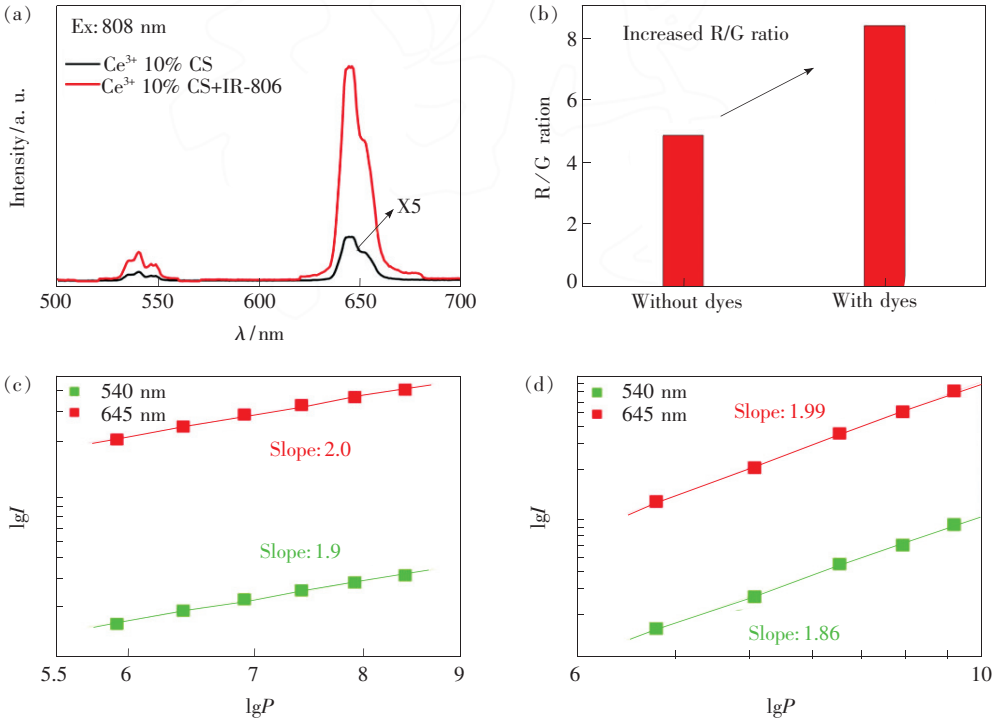


Fig. 4　(a) UC luminescence spectra of $NaYF_4$: Yb/Ho/Ce (20%/2%/10%) @ $NaYF_4$: Nd(20%) UCNPs (black line) and dye-sensitized UCNPs (red line). (b) Increased R/G ratio after conjugating UCNPs with dyes. Lg-lg plots of the UCL intensity *versus* laser power density for the green and red emissions of the UCNPs (c) and dye-sensitized UCNPs (d) under excitation of 808 nm.

## 4　Conclusion

In this work, highly uniform hexagonal phase $NaYF_4$: Yb/Ho/Ce (20%/2%/10%)@$NaYF_4$: Nd (20%) UCNPs were prepared by solvothermal method, and thus IR-806 molecules were successfully conjugated on the surface of UCNPs. By varying the $Ce^{3+}$ doping concentration (0% ~10%), the R/G of $Ho^{3+}$ gradually increased with the $Ce^{3+}$ doping concentration. Especially for 10% $Ce^{3+}$ doping concentration, a single-band red UC luminescence was achieved, though more than 90% of the total UCL intensity was quenched by $Ce^{3+}$ ions. After further surface conjugation with near-infrared IR-806 molecules, the luminescence intensity of the UCNPs was significantly increased by a factor of 22. More importantly, the R/G emission ratio of $Ho^{3+}$ increased from ~4.9 to 8.4. Therefore, the dye-sensitization method not only enhanced $Ho^{3+}$ single-band upconversion luminescence intensity, but also improved the red emission purity, which is beneficial to single-band red emission for high-resolution bioimaging.

**References:**


[1] DONG H,SUN L D,YAN C H. Energy transfer in lanthanide upconversion studies for extended optical applications [J]. *Chem. Soc. Rev.*, 2015,44(6):1608-1634.

[2] 于海洋,涂浪平,张友林,等. 溶剂中稀土上转换纳米粒子表面猝灭效应的定量分析 [J]. 中国光学, 2019,12(6):1288-1294.
YU H Y,TU L P,ZHANG Y L,*et al.*. Quantitative analysis of the surface quenching effect of lanthanide-doped upconversion nanoparticles in solvents [J]. *Chin. Opt.*, 2019,12(6):1288-1294. (in Chinese)

[3] CHEN B,WANG F. Combating concentration quenching in upconversion nanoparticles [J]. *Acc. Chem. Res.*, 2020, 53(2):358-367.

[4] 徐文,陈旭,宋宏伟. 稀土离子上转换发光中的局域电磁场调控 [J]. 发光学报, 2018,39(1):1-26.
XU W,CHEN X,SONG H W. Manipulation of local electromagnetic field in upconversion luminescence of rare earth ions [J]. *Chin. J. Lumin.*, 2018,39(1):1-26. (in Chinese)

[5] WEN S H,ZHOU J J,SCHUCK P J,*et al.*. Future and challenges for hybrid upconversion nanosystems [J]. *Nat. Photonics*, 2019,13(12):828-838.

[6] 贺飞,盖世丽,杨飘萍,等. 稀土上转换荧光材料的发光性质调变及其应用 [J]. 发光学报, 2018,39(1):92-106.
HE F,GAI S L,YANG P P,*et al.*. Luminescence modification and application of the lanthanide upconversion fluorescence materials [J]. *Chin. J. Lumin.*, 2018,39(1):92-106. (in Chinese)

[7] WANG D,XUE B,OHULCHANSKYY T Y,*et al.*. Inhibiting tumor oxygen metabolism and simultaneously generating oxygen by intelligent upconversion nanotherapeutics for enhanced photodynamic therapy [J]. *Biomaterials*, 2020, 251: 120088.

[8] 李晓晓,李蕴乾,汪欣,等. 高灵敏度下转换光学测温材料:$NaGd(WO_4)_2$:$Yb^{3+}$/$Er^{3+}$ [J]. 中国光学, 2019,12(3):596-605.
LI X X,LI Y Q,WANG X,*et al.*. Highly sensitive down-conversion optical temperature-measurement material: $NaGd(WO_4)_2$: $Yb^{3+}$/$Er^{3+}$ [J]. *Chin. Opt.*, 2019,12(3):596-605. (in Chinese)

[9] YANG Y M. Upconversion nanophosphors for use in bioimaging,therapy,drug delivery and bioassays [J]. *Microchim. Acta*, 2014,181(3-4):263-294.

[10] WANG F,WEN S H,HE H,*et al.*. Microscopic inspection and tracking of single upconversion nanoparticles in living cells [J]. *Light: Sci. Appl.*, 2018,7(4):18007.

[11] LIU X L,YAN L,LIU S B,*et al.*. Controllable synthesis of ultrasmall core-shell hexagonal upconversion nanoparticles towards full-color output [J]. *Optik*, 2020, 207:164398.

[12] WANG J,WANG F,WANG C,*et al.*. Single-band upconversion emission in lanthanide-doped $KMnF_3$ nanocrystals [J]. *Angew. Chem. Int. Ed.*, 2011,50(44):10369-10372.

[13] LIN H,XU D K,LI A M,*et al.*. Morphology evolution and pure red upconversion mechanism of β-$NaLuF_4$ crystals [J]. *Sci Rep.*, 2016,6:28051-1-12.

[14] TIAN G,GU Z J,ZHOU L J,*et al.*. $Mn^{2+}$ dopant-controlled synthesis of $NaYF_4$: Yb/Er upconversion nanoparticles for *in vivo* imaging and drug delivery [J]. *Adv. Mater.*, 2012,24(9):1226-1231.

[15] CHEN G Y,LIU H C,SOMESFALEAN G,*et al.*. Upconversion emission tuning from green to red in $Yb^{3+}$/$Ho^{3+}$-codoped $NaYF_4$ nanocrystals by tridoping with $Ce^{3+}$ ions [J]. *Nanotechnology*, 2009, 20(38):385704-1-6.

[16] WANG D,XUE B,KONG X G,*et al.*. 808 nm driven $Nd^{3+}$-sensitized upconversion nanostructures for photodynamic therapy and simultaneous fluorescence imaging [J]. *Nanoscale*, 2015,7(1):190-197.

[17] WANG D,XUE B,SONG J,*et al.*. Compressed energy transfer distance for remarkable enhancement of the luminescence of $Nd^{3+}$-sensitized upconversion nanoparticles [J]. *J. Mater. Chem.* C, 2018,6(24):6597-6604.

[18] ZOU W Q,VISSER C,MADURO J A,*et al.*. Broadband dye-sensitized upconversion of near-infrared light [J]. *Nat. Photonics*, 2012,6(8):560-564.

[19] XUE B,WANG D,TU L P,*et al.*. Ultrastrong absorption meets ultraweak absorption: unraveling the energy-dissipative routes for dye-sensitized upconversion luminescence [J]. *J. Phys. Chem. Lett.*, 2018,9(16):4625-4631.

[20] CHEN G Y,DAMASCO J,QIU H L,*et al.*. Energy-cascaded upconversion in an organic dye-sensitized core/shell fluoride

nanocrystal [J]. *Nano Lett.*, 2015,15(11):7400-7407.

[21] CHEN G Y,SHAO W,VALIEV R R,*et al.*. Efficient broadband upconversion of near-infrared light in dye-sensitized core/shell nanocrystals [J]. *Adv. Opt. Mater.*, 2016,4(11):1760-1766.

[22] XUE B,WANG D,ZHANG Y L,*et al.*. Regulating the color output and simultaneously enhancing the intensity of upconversion nanoparticles *via* a dye sensitization strategy [J]. *J. Mater. Chem.* C, 2019,7(28):8607-8615.

**王丹**(1986 - ),女,吉林松原人,博士,博士后,2015 年于中国科学院长春光学精密机械与物理研究所获得博士学位,主要从事发光材料设计及其生物医学应用的研究。
E-mail: wangdan66322@163.com

**孔祥贵**(1955 - ),男,山东曲阜人,博士,研究员,博士研究生导师,1998 年于中国科学院长春物理研究所获得博士学位,主要从事发光纳米材料在生物医学中应用的研究。
E-mail: xgkong14@ciomp.ac.cn

**宋军**(1978 - ),男,河北沧州人,博士,教授,博士研究生导师,2008 年于瑞典皇学工学院获得博士学位,主要从事纳米光子学、尤其是高分辨荧光成像技术在生物医学光学检测及新能源技术中应用的研究。
E-mail: songjun@szu.edu.cn